

Fabrication and characterization of Ge–Ga–Sb–S glass microsphere lasers operating at~1.9 μm

Kun Yang(杨坤), Shixun Dai(戴世勋), Yuehao Wu(吴越豪), Qiuhua Nie(聂秋华)

Citation: Chin. Phys. B . 2018, 27(11): 117701. **doi:** 10.1088/1674-1056/27/117701
Journal homepage: http://cpb.iphy.ac.cn; http://iopscience.iop.org/cpb

What follows is a list of articles you may be interested in

Square microcavity semiconductor lasers

YueDe Yang(杨跃德), HaiZhong Weng(翁海中), YouZeng Hao(郝友增), JinLong Xiao(肖金龙), YongZhen Huang(黄永箴)

Chin. Phys. B . 2018, 27(11): 114212. **doi:** 10.1088/1674-1056/27/11/114212

Effect of oxygen content on dielectric characteristics of Cr-doped $LaTiO_x$

Ming Ma(马铭), Yan Chen(陈彦), Yi-Min Cui(崔益民)

Chin. Phys. B . 2018, 27(5): 057702. **doi:** 10.1088/1674-1056/27/5/057702

Silica-based microcavity fabricated by wet etching

H Long(龙浩), W Yang(杨文), L Y Ying(应磊莹), B P Zhang(张保平)

Chin. Phys. B . 2017, 26(5): 054211. **doi:** 10.1088/1674-1056/26/5/054211

Indium-tin oxide films obtained by DC magnetron sputtering for improved Si heterojunction solar cell applications

Gu Jin-Hua, Si Jia-Le, Wang Jiu-Xiu, Feng Ya-Yang, Gao Xiao-Yong, Lu Jing-Xiao

Chin. Phys. B . 2015, 24(11): 117703. **doi:** 10.1088/1674-1056/24/11/117703

Stability and elastic properties of Nb_xC_y compounds

Gao Xu-Peng, Jiang Ye-Hua, Liu Yang-Zhen, Zhou Rong, Feng Jing

Chin. Phys. B . 2014, 23(9): 097704. **doi:** 10.1088/1674-1056/23/9/097704

Fabrication and characterization of Ge–Ga–Sb–S glass microsphere lasers operating at ∼1.9 μm*

Kun Yang(杨坤)[1], Shixun Dai(戴世勋)[1,2], Yuehao Wu(吴越豪)[1,2,†], and Qiuhua Nie(聂秋华)[1,2,‡]

[1] *Advanced Technology Research Institute, Laboratory of Infrared Materials and Devices, Ningbo University, Ningbo* 315211, *China*
[2] *Key Laboratory of Photoelectric Materials and Devices of Zhejiang Province, Ningbo* 315211, *China*

(Received 11 July 2018; revised manuscript received 16 August 2018; published online 24 October 2018)

We report the fabrication and characterization of germanium gallium antimony sulfide (Ge–Ga–Sb–S or 2S2G, doped with Tm^{3+} ions) microsphere lasers operating at ∼1.9-μm spectral band. Compared to the chalcogenide glasses that are used in previous microsphere lasers, this 2S2G glass has a lower transition temperature and a higher characteristic temperature. This implies that 2S2G microspheres can be fabricated at lower temperatures and the crystallization problem in the sphere-forming process can be alleviated. We show that hundreds of high-quality microspheres (quality factors higher than 10^5) of various diameters can be produced simultaneously via a droplet sphere-forming method. Microspheres are coupled with silica fiber tapers for optical characterizations. We demonstrate that Whispering Gallery mode (WGM) patterns in the 1.7–2.0 μm band can be conveniently obtained and that once the pump power exceeds a threshold, single- and multi-mode microsphere lasers can be generated. For a typical microsphere whose diameter is 258.64 μm, we demonstrate its laser threshold is 0.383 mW, the laser wavelength is 1907.38 nm, and the thermal sensitivity of the microsphere laser is 29.56 pm/°C.

Keywords: chalcogenides, microspheres laser, whispering gallery modes

PACS: 77.84.Bw, 42.55.Sa, 42.82.Et **DOI:** 10.1088/1674-1056/27/11/117701

1. Introduction

Mid-infrared (MIR) lasers play an important role in many modern industrial, military, and medical applications.[1–3] Recently, MIR microsphere lasers have attracted special interest because of their many desirable properties, such as low pump thresholds, narrow linewidths, compact sizes, and low fabrication costs. Novel infrared materials such as tellurite, ZBLAN, and chalcogenide glasses are used to fabricate microsphere lasers operating in the MIR spectral region. For instance, Sasagawa *et al*. used a Tm^{3+}-doped tellurite glass as the base material to build microsphere lasers operating near 1.9 μm.[4] Vanier *et al*. improved the quality of tellurite glass microspheres and reduced the laser thresholds to a few microwatts.[5] Yang *et al*. built ∼2.1-μm microsphere lasers with a Tm^{3+}–Ho^{3+} co-doped tellurite glass.[6] Behzadi *et al*. reported a 2.71-μm microsphere laser based on an Er^{3+}-doped ZBLAN glass.[7–9]

Chalcogenide glasses are also promising base materials for MIR microsphere lasers.[10] Compared to the tellurite and ZBLAN glasses, chalcogenide glasses have much wider transmission windows and thus can potentially support more operation wavelengths for microsphere lasers. Elliott *et al*. reported one of the earliest chalcogenide glass microsphere lasers, which was based on a gallium lanthanum sulfide (GLS) glass. This microsphere laser used Nd^{3+} ions as active dopants and operated in the ∼1.0-μm band.[11] We previously proposed using a germanium gallium sulfide (GGS) glass to build microsphere lasers.[12] Compared to the GLS glass, the GGS glass has a lower melting temperature and thus the sphere-forming temperature can be reduced. Vanier *et al*. reported a passive chalcogenide glass (As_2S_3) microsphere laser whose operation was based on the nonlinear optical mechanism of stimulated Raman scattering (SRS).[13]

In this work, we experimentally demonstrate that an alternative chalcogenide glass, germanium gallium antimony sulfide ($Ge_{20}Ga_5Sb_{10}S_{65}$, or 2S2G), can also be used to build microsphere lasers. Compared to the GLS glass, the transition temperature of the 2S2G glass is considerably lower. 2S2G microspheres can be formed at about 650 °C, whereas GLS microspheres need to be formed at near 1000 °C.[11] Compared to the GGS glass, the characteristic temperature of the 2S2G glass is higher by ∼40 °C, meaning that the crystallization problem in the sphere-forming process can be effectively mitigated. Compared to the As_2S_3 glass, this 2S2G glass is more environmentally friendly and is more feasible to dopant ions. We have reported the fabrication of active 2S2G microsphere resonators in a previous work.[14] However, we were limited by the quality of microspheres and were un-

*Project supported by the National Natural Science Foundation of China (Grant No. 61605094), the Key Program of National Natural Science Foundation of China (Grant No. 61435009), the Natural Science Foundation of Zhejiang Province, China (Grant No. LQ15F050002), and K. C. Wong Magna Fund in Ningbo University, China.

†Corresponding author. E-mail: wuyuehao@nbu.edu.cn
‡Corresponding author. E-mail: nieqiuhua@nbu.edu.cn

© 2018 Chinese Physical Society and IOP Publishing Ltd

able to obtain microsphere laser modes at that time. In this work, we improve the quality of 2S2G microspheres by elongating the length of the sphere-forming heating chamber. Additional heating time is provided to glass powders to complete their transformations into microspheres, so that larger and better quality (higher quality factor (Q factor)) microspheres can be obtained in this work. We present Q-factor measurements and WGM characterizations of high-quality microspheres fabricated in this work. We also demonstrate that once the pump power exceeds a threshold, microsphere laser modes can be generated. As a representative example, we demonstrate that for a 258.64-μm-diameter microsphere, the laser threshold is 0.383 mW, the laser wavelength is 1907.38 nm, and the thermal sensitivity of the microsphere laser is 29.56 pm/°C.

2. Experiments and discussion

We employed a droplet sphere-forming method to form 2S2G microspheres in a previous work.[14] In the droplet method, glass powders are dropped through a vertical heating chamber, wherein those powders are melted and transformed into microspheres by surface tension. For the case of forming chalcogenide glass microspheres, the heating chamber needs to be purged with inert gas, so that chalcogenide glass powders can be thermally processed without interacting with air molecules. In our previous work, the vertical chamber was built with off-the-shelf components in our laboratory. However, the design of that chamber was not ideal and its temperature settings were difficult to adjust. In this work, we customized a commercial furnace (Sante Inc., model number: STGK-40-12) to implement the droplet sphere-forming method. Based on our previous experience with the droplet method, we doubled the length of the heating chamber and reduced the chamber diameter by 1/3. Consequently, the thermal processing time of glass powders can be elongated and the uniformity of the chamber temperature can be improved.

Figure 1(a) shows a microscopy image of a typical batch of large (diameters larger than 200 μm) 2S2G microspheres and figure 1(b) shows an SEM image presenting a large microsphere (diameter: 266.05 μm) along with a small one (diameter: 87.57 μm). The green circle in Fig. 1(a) represents an ideal sphere. In these figures, we can visually evaluate that both the large and small microspheres have good surface quality and sphericity. Microspheres are then picked out and coupled with silica fiber tapers for optical characterizations. Figure 1(c) shows typical transmission spectra of the microsphere/fiber taper coupling system, captured with a large microsphere (diameter: 252.45 μm, in dotted black line) and a small microsphere (diameter: 80.63 μm, in solid red line) when coupled with a 1.83-μm waist-diameter silica fiber taper.

In Fig. 1(c), we can see that both the larger and small microspheres generate transmission spectra that contain deep, sharp, and periodic resonant dips. The arrows in this figure point to resonant dips that have Q-factors higher than 10^5. Compared to microspheres fabricated in our previous work, whose Q-factors are typically $\sim 10^4$, we can see our current 2S2G microspheres generate transmission spectra containing considerably more high-Q resonant dips, demonstrating the superior quality of current microspheres to the previous results. In Fig. 1(c), we can also note that the large microsphere generates a denser distribution of resonant dips than the small microsphere. This phenomenon is in accordance with the theoretical model proposed in Refs. [15] and [16]. According to that theory, within the same spectral range, large microspheres generate more resonant dips than smaller microspheres. For instance, for a 250-μm-diameter 2S2G microsphere in the spectral band of 1550–1560 nm, seven resonating dips for fundamental TE WGMs ($n = 1$, $m = l$, where n, m, and l represent the radial, azimuthal, and polar mode numbers of WGMs) can be existent, whose l mode numbers are 1120 (resonating at 1550.51 nm), 1121 (1551.87 nm), ..., 1126 (1558.73 nm), respectively. However, for a 100-μm diameter microsphere, only three resonating dips can be existent, whose l mode numbers are 442 (resonating at 1551.35 nm), 443 (1554.78 nm), and 444 (1558.23 nm).

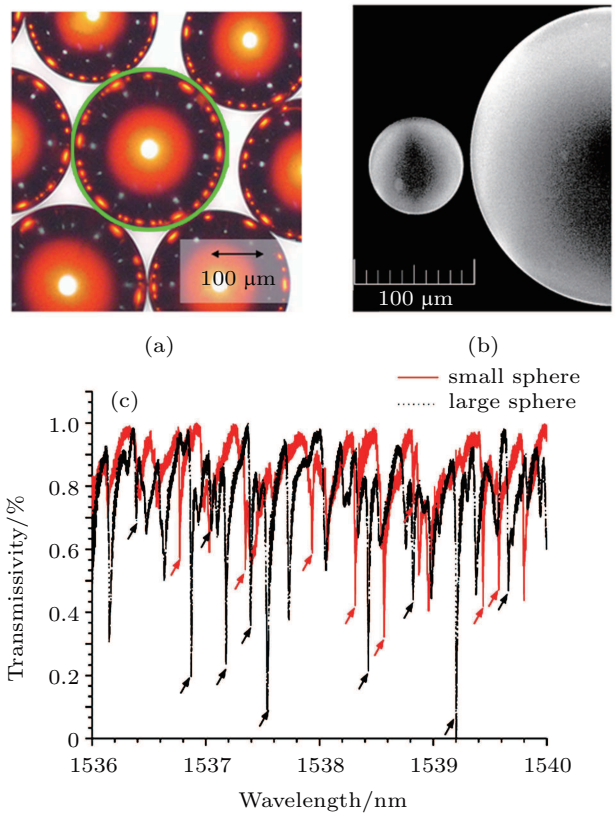


Fig. 1. (color online) (a) Microscopy image and (b) SEM image of typical 2S2G microspheres fabricated in this work. The green circle in (a) represents the contour of an ideal sphere. (c) Transmission spectra obtained with a 252.45-μm-diameter microsphere (black curve) and an 80.63-μm-diameter microsphere (red curve) when coupled with a 1.83-μm waist-diameter fiber taper. Red and black arrows in Fig. 1(c) point to resonant dips whose Q-factors are higher than 10^5.

3. Results

To excite fluorescence light in microspheres, an 808-nm laser diode (Changchun New Industrial Optoelectronics Tech. Co., model: MDL-III-808L/1–100 mW) is used as the pump source, which facilitates Tm^{3+} ions to transit from its base energy level ($^3H_6$) to a higher energy level ($^3H_4$). Tm^{3+} ions then undergo spontaneous $^3H_4$–$^3F_4$ and $^3F_4$–$^3H_6$ transitions, which result in fluorescence light in ∼1.47-μm and ∼1.90-μm bands, respectively. The fluorescence light is then evanescently coupled back into the fiber taper and is collected by an Optical Spectrum Analyzer (OSA, Yokogawa, model: AQ6375) and an infrared photodetector (Thorlabs, model: PDA10CS-EC) for spectral and power analyses. A schematic drawing of the experimental setup is shown in Fig. 2.

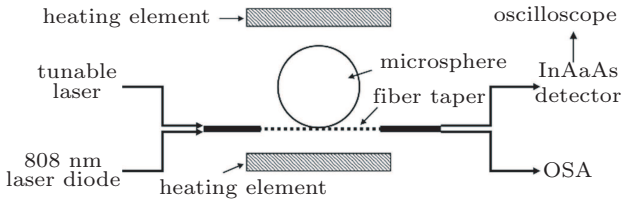


Fig. 2. Schematic drawing of the experimental setup.

Fluorescence light caused by spontaneous transitions of dopant ions propagates inside microspheres and forms WGM patterns in the transmission spectrum of the microsphere/fiber taper coupling system. Figure 3 shows the transmission spectra of the coupling system when a 258.64-μm diameter microsphere (red curve) and a 96.23-μm diameter microsphere (blue curve) are coupled with a 1.83-μm waist-diameter fiber taper. The same amount of pump power is employed when capturing these two spectral curves.

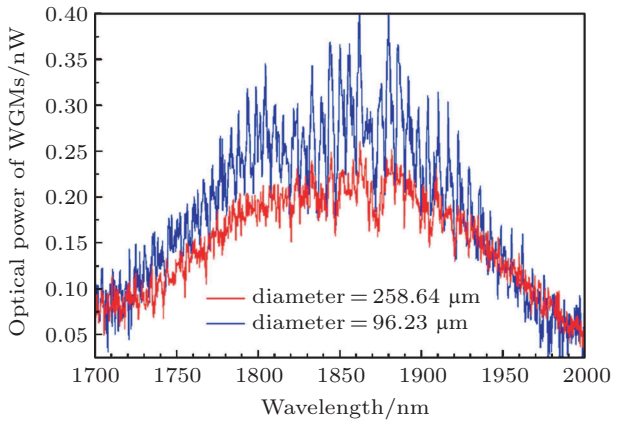


Fig. 3. (color online) Transmission spectra of the microsphere/fiber taper coupling system captured when a 258.64-μm diameter microsphere and a 96.23-μm diameter microsphere are coupled with a 1.83-μm waist-diameter fiber taper.

In the transmission spectra shown in Fig. 3, we can see oscillating intensity peaks and valleys, indicating the occurrences of various WGMs in those microspheres. We can also see that intensity variations in the red curve is less significant than those in the blue curve. This happens because larger microspheres generate WGMs with finer modal details than smaller ones and those finer details are less accurately resolved in spectral measurements due to the limited resolution of the OSA (0.05 nm).[16] It can also be noted that the larger microsphere outputs WGMs with lower powers than the smaller microsphere. This happens because the larger microsphere is in a less ideal phase-match condition with the silica fiber taper, which affects the efficiency of energy transfer between the microsphere and the fiber taper.[17]

In Fig. 4, we show the threshold behavior of a typical microsphere, whose diameter is 258.64 μm. In this figure, the output power of the microsphere laser is plotted as a function of the absorbed pump power. The absorbed pump power is measured as $W_{\text{out-of-contact}}$–$W_{\text{in-contact}}$, where $W_{\text{out-of-contact}}$ represents the pump power measured by the photodetector when the microsphere is not in contact with the fiber taper and $W_{\text{in-contact}}$ represents the pump power measured when the microsphere is in contact with the fiber taper.

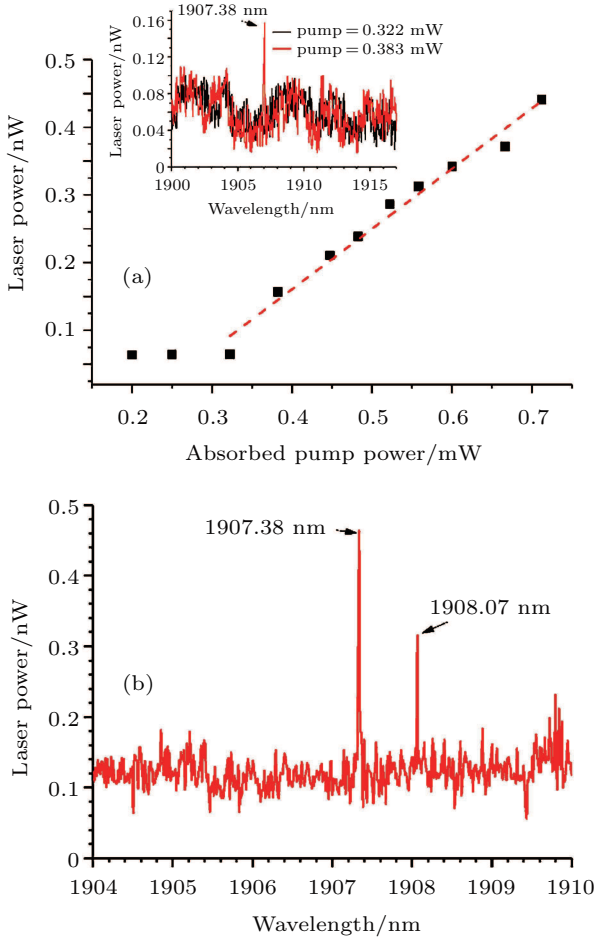


Fig. 4. (color online) Relationship between the output laser power and the absorbed pump power obtained with a 258.64-μm-diameter microsphere. The inset shows spectral measurements of the coupling system when the pump powers are 0.322 mW (black curve) and 0.383 mW (red curve). (b) Multi-mode microsphere laser obtained when the pump power increases to 0.712 mW.

In Fig. 4(a), we can see that as we increase the pump power, a laser threshold appears at 0.322 mW. In the inset of Fig. 4(a), we can see the onset of a single-mode laser when the pump power increases beyond the threshold of 0.322 mW to 0.383 mW. As we increase the pump power further beyond the laser threshold, the output power of the single mode laser increases as a linear function. At the pump power of 0.712 mW, the single-mode laser becomes a multi-mode one, as shown in Fig. 4(b), wherein a secondary lasing peak at 1908.07 nm can be noted.

To characterize the thermal response of 2S2G microsphere lasers fabricated in this work, we install the microsphere/fiber taper coupling system in a custom-made heating chamber. The heating chamber is essentially a "U" shaped copper plate equipped with metal ceramic heaters (MCHs) and thermal couples. When implementing the heating experiment, we carefully install the coupling system in between the two arms of the "U" shaped copper plate and raise the temperature of MCHs. A spectral shift from 1907.38 nm to 1909.39 nm can be noted as we increase the chamber temperature from 27 °C to 95 °C. Figure 5(a) shows microsphere lasers obtained at different temperatures and figure 5(b) shows the laser wavelength as a function of the environmental temperature.

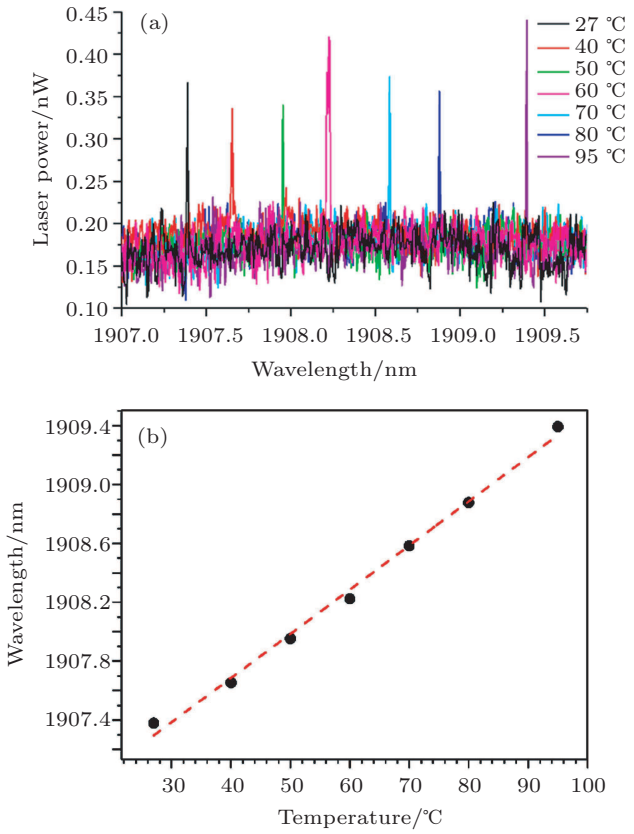


Fig. 5. (color online) (a) Thermal shift of the 2S2G microsphere laser. (b) Relationship between the laser wavelength and the environmental temperature.

A thermal sensitivity ($d\lambda/dT$) of 29.56 pm/°C can be derived from this result. Theoretically, the thermal sensitivity of microsphere lasers can be modeled as: $d\lambda/dT = \lambda_0(\alpha+\beta/n)$, where λ_0 is the laser wavelength of the microsphere at room temperature, α and β are the thermal expansion coefficient and coefficient of thermal refraction of the base material,[18] and n is the refractive index of the base material, which is 2.258 for the case of 2S2G glass. The thermal sensitivity of 2S2G microspheres was theoretically estimated to be 26 pm/°C in Ref. [14], which is similar to the experimentally measured value. Compared to microspheres fabricated with materials that have smaller thermal expansion coefficients or coefficient of thermal refractions, such as silver iodide microspheres (with a thermal sensitivity of 9.2 pm/°C[19]), the thermal response of the 2S2G glass microsphere is more attractive for practical applications. The thermal resolution ($\Delta T_{\min}$) of the 2S2G microsphere laser can be determined as the ratio between the linewidth of the microsphere laser ($\Delta\lambda_{\min}$) and its thermal sensitivity: $\Delta T_{\min} = \Delta\lambda_{\min}/(d\lambda/dT)$.[20] In this work, $\Delta\lambda_{\min}$ is determined by the spectral resolution of the OSA, which is 0.05 nm. Therefore, the thermal resolution of the current 2S2G microsphere laser is 1.69 °C. We can see that the 2S2G microsphere laser is sensitive to temperature variations. Therefore, in real application settings, it is important to utilize supplementary temperature controlling mechanisms to maintain a stable operating temperature for 2S2G microsphere lasers.

4. Conclusion

We demonstrate the fabrication and characterization of chalcogenide glass microsphere lasers operating at the ~1.9-μm spectral band. A Tm^{3+}-doped 2S2G glass is used as the base material and a droplet method is employed to mass-produce microspheres. Compared to our previous work, we improve the quality of 2S2G microspheres by increasing the length of the heating chamber, which provides additional heating time for the glass powders to complete their sphere-forming process. We demonstrate that both large and small microspheres fabricated in this work generate high-Q ($\sim 10^5$) resonant dips in their transmission spectra. For a typical 2S2G microsphere with a diameter of 258.64 μm, we demonstrate that its laser wavelength is 1907.38 nm, the laser threshold is 0.383 mW, and the thermal sensitivity of the laser is 29.56 pm/°C. This work implies that this 2S2G glass can be considered as a promising base material for various active optical/photonic devices that operate in the MIR spectrum.

References

[1] Tao M, Tao B, Hu Z, Feng G, Ye X and Zhao J 2017 *Opt. Exp.* **25** 32386
[2] Behzadi B, Aliannezhadi M, Hossein-Zadeh M and Jain R K 2017 *J. Opt. Soc. Am. B* **34** 2501
[3] Huang H, Wang H and Shen D 2017 *Opt. Mater. Express* **7** 3147
[4] Sasagawa K, Yonezawa Z, Iwai R, Ohta J and Nunoshita M 2004 *Appl. Phys. Lett.* **85** 4325

[5] Vanier F, Cote F, Amraoui M E, Messaddeq Y, Peter Y A and Rochette M 2015 *Opt. Lett.* **40** 5227

[6] Yang Z, Wu Y, Yang K, Xu P, Zhang W, Dai S and Xu T 2017 *Opt. Mater.* **72** 524

[7] Behzadi B, Jain R K and Hossein-Zadeh M 2017 *IEEE J. Quantum Electron.* **53** 5700109

[8] Behzadi B, Jain R K and Hossein-Zadeh M 2018 *Laser Phys. Lett.* **15** 085112

[9] Deng Y, Jain R K and Hossein-Zadeh M 2014 *Opt. Lett.* **39** 4458

[10] Eggleton B J, Luther-Davies B and Richardson K 2011 *Nat. Photon.* **5** 141

[11] Elliott G R, SenthilMurugan G, WilkinsonJ S, Zervas M N and Hewak D W 2010 *Opt. Express* **18** 26720

[12] Li C, Dai S, Zhang Q, Shen X, Wang X, Zhang P, Lu L, Wu Y and Lv S 2015 *Chin. Phy. B* **24** 044208

[13] Vanier F, Peter Y A and Rochette M 2014 *Opt. Express* **22** 28731

[14] Yang Z, Wu Y, Zhang X, Zhang W, Xu P and Dai S 2017 *IEEE Photon. Technol. Lett.* **29** 66

[15] Schiller S 1993 *Appl. Opt.* **32** 2181

[16] Lam C C, Leung P T and Young K 1992 *J. Opt. Soc. Am. B* **9** 1585

[17] Wang P, Lee T, Ding M, Dhar A, Hawkins T, Foy P, Semenova Y, Wu Q, Sahu J, Farrell G, Ballato J and Brambilla G 2012 *Opt. Lett.* **37** 728

[18] Peng X, Song F, Kuwata-Gonokami M, Jiang S and Peyghambarian N 2003 *Appl. Phys. Lett.* **83** 5380

[19] Milenko K, Konidakis I and Pissadakis S 2016 *Opt. Lett.* **41** 2185

[20] Dong C H, He L, Xiao Y F, Gaddam V R, Ozdemir S K, Han Z F, Guo G C and Yang L 2009 *Appl. Phys. Lett.* **94** 231119